**Original Research Article****Production of Modified Superplasticizer by Two-Step Synthesis of Nanosilica-Polycarboxylate Ether**Alireza Taheri^{1, 2*} , Alireza Jafari³ , Fatemeh Jafari⁴ ¹Department of Chemistry, Ilam Branch, Islamic Azad University, Ilam, Iran²Arta Shimi Alborz Technical, Engineering, Educational and Research Institute, Tehran, Iran³Department of Polymer Engineering, Islamic Azad University, South Tehran, Tehran, Iran⁴ Department of Civil Engineering, Technische Universität München, Lichtenbergstrasse 4, Garching 85748, Germany**ARTICLE INFO****ARTICLE HISTORY****Submitted:** 2023-10-07**Revised:** 2023-12-05**Accepted:** 2023-12-25**Available online:** 2023-12-31**Manuscript ID:** AJCB-2310-1201**Checked for Plagiarism:** Yes**Language Editor:** Dr. Fatimah Ramezani**Editor who Approved****Publication:** Dr. Esmail Doustkhah**KEY WORDS**

Superplasticizers
 Polycarboxylate ether
 Solution synthesis
 Nanosilica

ABSTRACT

The impact of adding nanosilica (NS) and polycarboxylate-ether plasticizer (PCE) admixtures was examined individually and in combination to aerial lime mortars. The inclusion of NS alone resulted in an increase in water demand, as evidenced by the mini-spread flow test. Through particle size distribution studies, zeta potential measurements, and optical microscopy, it was observed that an interaction occurred between NS and hydrated lime particles in fresh mixtures, leading to the formation of agglomerates. This synthesis was performed at three different temperature levels, and the resulting product underwent FTIR analysis to verify its structure. Furthermore, an HNMR test was conducted to confirm the completion of the final synthesis. To determine the characteristics of the synthesized polycarboxylate ether, including the average molecular weight and molecular weight distribution curve, a GPC analysis (Gel permeation chromatography) was carried out. The MW and PDI (polydispersity index) values were reported, and finally, a slump test was performed to confirm the performance of the synthesized product. The length of the main chain in the copolymer increases as the synthesis temperature rises. This increase is more pronounced at higher temperatures. However, temperatures exceeding 70 °C can lead to the destruction of the copolymer, resulting in a decrease in viscosity and a change in the solution color. Therefore, it is recommended to carry out the primary synthesis at 70 °C for 8 hours.

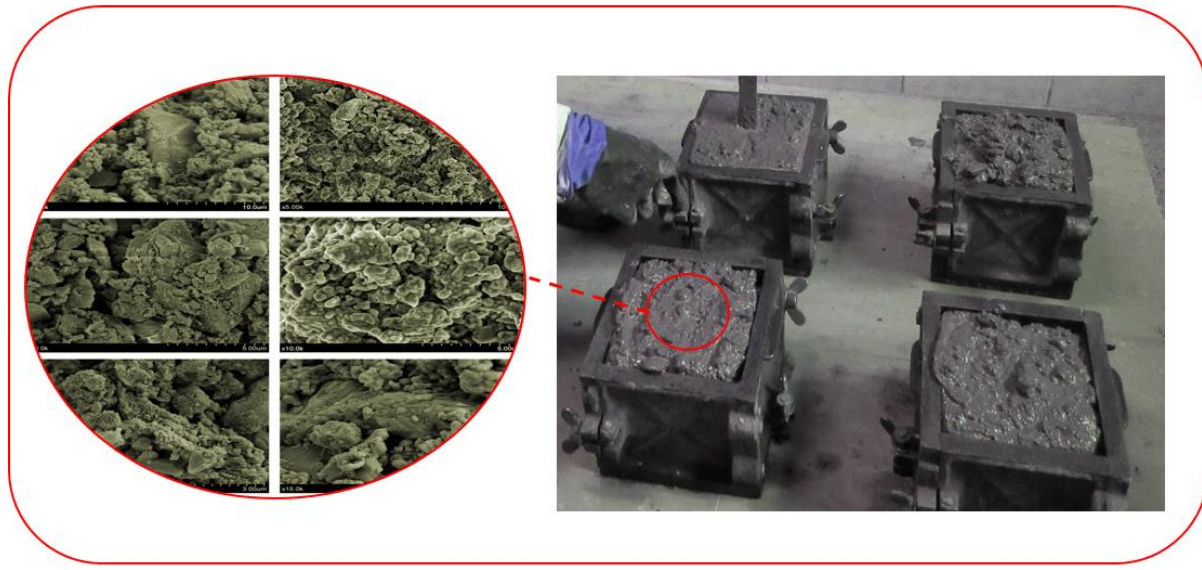
Citation: Alireza Taheri, Alireza Jafari, Fatemeh Jafari, Production of Modified Superplasticizer by Two-StepSynthesis of Nanosilica-Polycarboxylate Ether, *Adv. J. Chem. B*, 6 (2024) 31-45.<https://doi.org/10.48309/ajcb.2024.419761.1201>https://www.ajchem-b.com/article_186586.html

* Corresponding author: Alireza Taheri

✉ E-mail: alireza.taheri@iau.ac.ir, alirezachem@yahoo.com

© 2024 by SPC (Sami Publishing Company)

GRAPHICAL ABSTRACT

**Introduction**

Concrete is a widely utilized construction material that serves as the foundation of modern life. As concrete technology has advanced, additives have been developed and employed to impart specific properties to concrete [1]. These additives can be categorized into two groups: mineral additives and chemical additives [2]. Chemical additives play various roles in enhancing the concrete quality in both its fresh and hardened states. In fresh concrete, chemical additives are used to improve properties such as increasing fluidity and workability without the need for additional water, or reducing the water content without compromising the concrete's flow and workability. They can also delay or accelerate the initial setting time, minimize or prevent shrinkage and cracking, adjust sweating properties, reduce segregation, enhance pumpability, mitigate slump effects, and improve finishing capabilities. Furthermore, chemical additives can decrease the rate of heat release during the initial cement hydration, enhance early-stage strength development,

increase overall strength (compressive, tensile, or flexural), improve resistance to freezing and thawing, reduce permeability, mitigate expansion caused by alkaline reactions, enhance adhesion to steel and existing concrete, improve impact resistance and wear resistance, inhibit corrosion of embedded metals, facilitate the production of colored concrete or mortar, and minimize erosion during drying [3]. Chemical additives have played a crucial role in reducing water usage and increasing the strength of concrete production. These additives can be categorized into three generations. The first generation includes lubricants such as Sulfonated naphthalene formaldehyde salts, which can reduce water usage by up to 15%. The second generation includes excellent lubricants like melamine formaldehyde sulfonate salts, which can reduce water usage by up to 25%. The third generation includes superplasticizer like polymeric superplasticizer based on polycarboxylate ether, which can reduce water usage by up to 40%. With the increasing demand for concrete and industrial ceramics, lubricants have become increasingly important. Among the

third-generation chemical super-lubricants, polycarboxylate ether holds great significance and application. Researchers like Host *et al.* [5] have studied the rheology of lubricants, while Nava [6] has focused on the effect mechanism of copolymer additives as a super-lubricant for concrete. Vinefeld *et al.* [7] conducted a study on the impact of lubricants featuring a shoulder structure. Ran *et al.* [8] assessed the length of side chains in copolymers that were added to concrete. Roy Ping *et al.* [9] synthesized samples of polycarboxylate ether as a superplasticizer. Rong Ping *et al.* [10] investigated the performance of polycarboxylate ether as a concrete super-lubricant. Jian Hu *et al.* [11] focused on the synthesis mechanism of polycarboxylate ether and its ability to reduce water usage in concrete. Shan *et al.* [12] examined the influence of the molecular weight of polycarboxylate ether used in concrete. Lee *et al.* [13] investigated the impact of polyethylene oxide chains on the effectiveness of polycarboxylate in reducing water content in concrete. X Ping and Hui [14] focused on the influence of side chains of polycarboxylate lubricant on cement hydration. Baogwao *et al.* [15] examined the effect of superdensity of polycarboxylate lubricant and its side chains. Ixo Qiuing *et al.* [16] evaluated the spreading ability of cement particles using carboxylate copolymers. Jane May *et al.* [17] made modifications to the structure of polycarboxylate ether to enhance its superplasticizing properties. Ben Vy *et al.* [18] described the correlation between the structure and performance of polycarboxylate superplasticizer samples. Axioxing [19] proposed novel synthesis methods for polycarboxylate lubricants. Moix *et al.* [20] classified the characteristics and applications of polycarboxylates in concrete. Building upon the previous research, this article investigates the first two-step synthesis of polycarboxylate ether using mass and solution methods, with a focus on the temperature factor in this synthesis. The

first stage involves the creation of the main chain, while the second stage involves the formation of secondary chains. The reaction temperature is carefully controlled to monitor the progress of the reaction in these stages.

Experimental Materials

The substances employed encompass acrylic acid (AA), (AIBN, azobisisobutyronitrile), 3-chloro-2-methyl-1-propene (CMP), polyethylene glycol with an average molecular weight (PEG-1000), potassium carbonate, and ethanol. All of the materials were procured from Merck Company.

Preparation of samples

Initially, 2.7 g (8.6 ml) of acrylic acid and 0.001 g of initiator (AIBN azobis isobutyronitrile) were carefully measured and poured into a flask with four openings. Subsequently, 9 g (7.9 ml) of alkyl halide, specifically 3-chloro-2-methyl-1-propene, were added drop by drop at a very slow rate through one of the openings into the flask. The flask, containing the mixture, was then placed on a magnetic stirrer and immersed in an oil bath made of paraffin. To ensure proper monitoring, a thermometer was inserted into one of the openings of the flask, while a condenser was installed in another opening. The third opening was used to release any gas and prevent oxygen entry. The temperature was carefully set at 60, 50, and 70 °C. It is worth noting that exceeding the temperature of 70 °C would result in the copolymer destruction. Initially, the product appeared colorless, but over time and after 8 hours of reaction, the solution gradually changed its color to pale yellow and eventually dark yellow, indicating the completion of the reaction. Based on the reaction's stoichiometry and the weight of raw materials used, 0.1 mol of the raw materials were weighed, and the molar ratios of 0.1 were maintained to ensure equal proportions in the reaction.

The copolymer was combined with 5 g of polyethylene glycol and 0.138 g of potassium carbonate as catalyst. The mixture was then placed on a magnetic stirrer. To facilitate the dissolution of the copolymer and polyethylene glycol, ethanol solvent was added, and the polymerization was carried out in solution form. As the reaction progressed and heat was applied, the ethanol solvent gradually evaporated and escaped from the reaction environment. The synthesis temperature ranged from 50 to 70 °C, and the reaction time lasted for 6 hours. At this stage, the raw materials were weighed based on the stoichiometry of the reaction, resulting in a total of 0.1 mol of raw materials and molar ratios of 0.1.

Mortar preparation

To prepare the mortar, a solid admixtures mixer BL-8-CA (Lleal S.A.) was used to blend lime, aggregate, and dry sample admixture for 5 minutes. Water and 0.5 - 1wt% nanosilica suspension were then added and mixed for 90 seconds at low speed using a Proeti ETI 26.0072 mixer. The mortars were left to settle for 10 minutes before analyzing fresh state properties. For hardened state properties, the mortars were molded in prismatic 40x40x160 mm casts, compacted in a specific automatic compactor for 60 seconds, and stored indoors at 25 °C. They were demolded 5 days later and tested after 7 curing days. The results were statistically significant as three specimens were tested at each time for each sample, and the reported results are an average of the obtained results.

Instruments

The synthesized material's structural groups were investigated using a Fourier transform infrared spectrometer - Bruker, Tensor 27 (Germany). The viscosity of the polymer solution was measured using a viscometer of Ubbelhode glasses. To determine the concrete mixing plan and measure the flow of concrete, the slump test

according to Iran's national standard No. 3519 was utilized. For nuclear magnetic resonance spectrometry (NMR), a 500 MHz NMR device manufactured by Bruker, Germany, was used with deuterium dimethyl sulfoxide (DMSO) solvent. Gel permeation chromatography (GPC) was performed using a Series 110 device from Agilent.

Results and Discussion

The copolymerization of the initial copolymer was conducted using equal molar ratios and under identical synthesis conditions. However, the synthesis was performed at varying temperatures in order to examine the impact of reaction temperature on the resulting copolymer. The copolymer synthesis was achieved through the mass method and free radical mechanism, with the objective of forming the primary structure of polycarboxylate ether (see Fig 1 for the reaction formula).

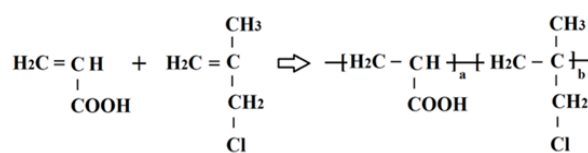


Fig. 1.Mechanism of copolymer synthesis for the primary polycarboxylate ether chain

To identify the functional groups formed as predicted and to obtain the copolymer, an FTIR analysis was conducted. Fig 2 displays the FTIR spectrum of the synthesized samples at three different temperature levels (60, 50, and 70 °C) with a reaction time of 8 hours and molar ratios of 0.1 and equal. The codes of production samples in the first stage of synthesis are presented in Table 1. The synthesized polymers exhibited identical spectra. Each peak in the FTIR spectrum represents a bond or functional group, such as the O-H bond peak in the 3500 cm⁻¹ region, the C-H bond peak in the 3000 cm⁻¹ region, and the C-C bond peak in the 1000 cm⁻¹ region. Observations were made of a C=C

aliphatic bond peak at 1700 cm^{-1} and a C-O bond peak at 1100 cm^{-1} . Figure 2d displays a diagram comparing the three obtained spectra, highlighting the matching of specific peaks. The relative viscosity of the copolymer was then determined as a parameter for assessing the progress of the chain length and process for all three conditions, with the results presented in **Table 2**. As the main chain of the copolymer increased, so did its relative viscosity at high temperatures. However, at over $70\text{ }^{\circ}\text{C}$, changes in color and a drop in relative viscosity indicated the beginning of chain destruction. In the second phase, sample S3 was used to synthesize polycarboxylate ether. During this step, the synthesis temperature was varied across three different levels while maintaining the same synthesis conditions. The synthesized polycarboxylate ether was initially analyzed using FTIR. In addition, the structure and HNMR test were conducted to confirm the successful synthesis of polycarboxylate ether. Subsequently, the GPC test was performed to determine the characteristics of the synthesized polycarboxylate ether, including the average molecular weight of the polymer and the molecular weight distribution curve. The values of MW and PDI were reported as a result of this test. Finally, the slump test was carried out to verify the performance of the synthesized polycarboxylate ether. The synthesis of polycarboxylate ether was conducted using equal molar ratios and consistent synthesis conditions, with the only variation being the different temperatures. This was done to investigate the impact of reaction temperature on the resulting polycarboxylate ether. The objective of this study was to synthesize

polycarboxylate ether side chains through condensation polymerization by solution method. The reaction formula is depicted in **Fig 3** and the resulting structure was confirmed through FTIR analysis. **Fig 4** displays the FTIR spectra of the synthesized samples at three different temperature levels (60 , 50 , and $70\text{ }^{\circ}\text{C}$) with a reaction time of 6 hours and molar ratios of 0.1 and 1 . The code of the tested samples is presented in **Table 3**. By comparing the three obtained spectra in a diagram, as demonstrated in **Fig 4**, the matching of specific peaks can be observed [21-28].

Table 1. Instruments and analysis techniques employed to investigate the impact of nanosilica on the subject

Sample No.	The first synthesis step conditions (copolymer synthesis -main chain created)
S1	Temperature: $50\text{ }^{\circ}\text{C}$, Reaction Time : 8 h Equal mole fraction of AA and CMP
S2	Temperature: $60\text{ }^{\circ}\text{C}$, Reaction Time : 8 h Equal mole fraction of AA and CMP
S3	Temperature: $70\text{ }^{\circ}\text{C}$, Reaction Time : 8 h Equal mole fraction of AA and CMP

Table2. Copolymer synthesis relative viscosity in different temperature

Sample No.	Relative Viscosity (Solute discharge time / Solvent discharge time)
S1	12.54
S2	16.45
S3	21.34

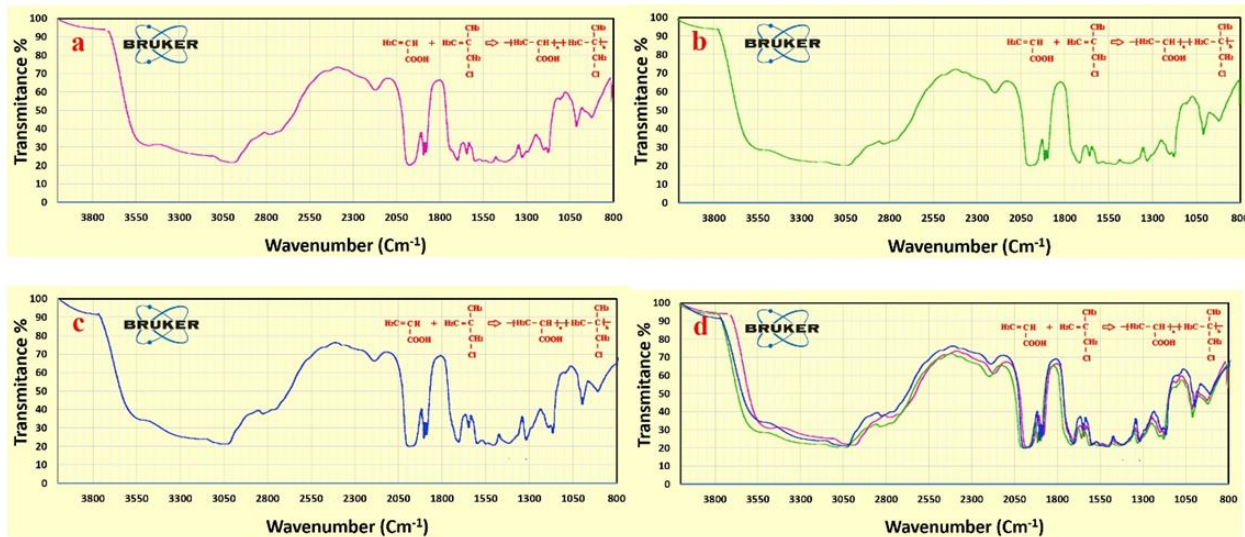


Fig. 2.FTIR spectra of primary copolymer synthesis, FTIR spectrum of sample S1 (a), sample S2 (b), sample S3 (c), and comparison of FTIR spectra (d)

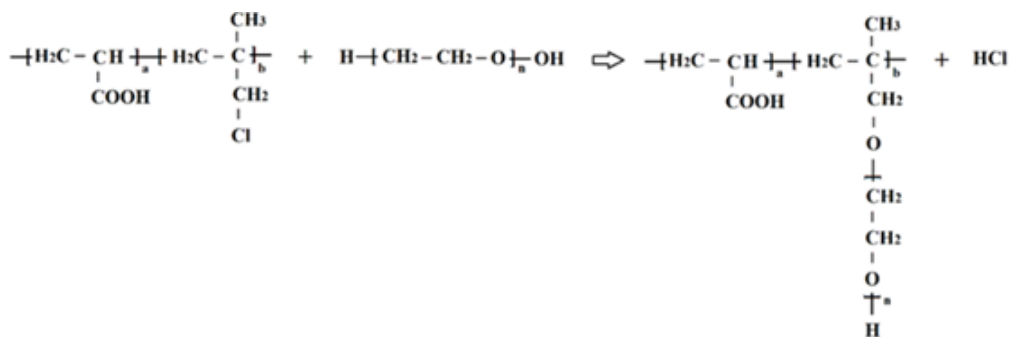


Fig. 3. Mechanism of synthesized polycarboxylate ether and created side chain

Table3. In the second step of synthesis, a sample coding is performed to create a side chain of synthesized polycarboxylate ether

Sample No.	Synthesized polycarboxylate ether – created side chain
S31	Temperature: 50 °C, Reaction Time : 8 h Equal mole fraction of S3 and PEG
S32	Temperature: 60 °C, Reaction Time : 8 h Equal mole fraction of S3 and PEG
S33	Temperature: 70 °C, Reaction Time : 8 h Equal mole fraction of S3 and PEG

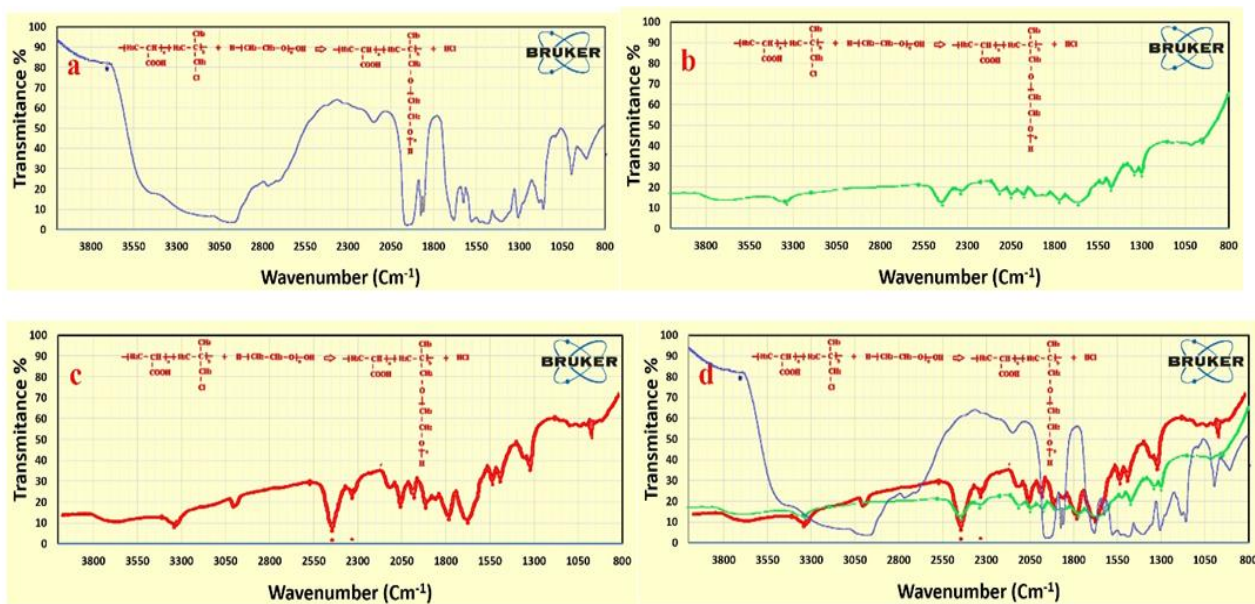


Fig 4.FTIR spectra of synthesized polycarboxylate ether, Sample S31 (a), sample S32 (b), sample S33 (c), and comparison of FTIR spectra (d)

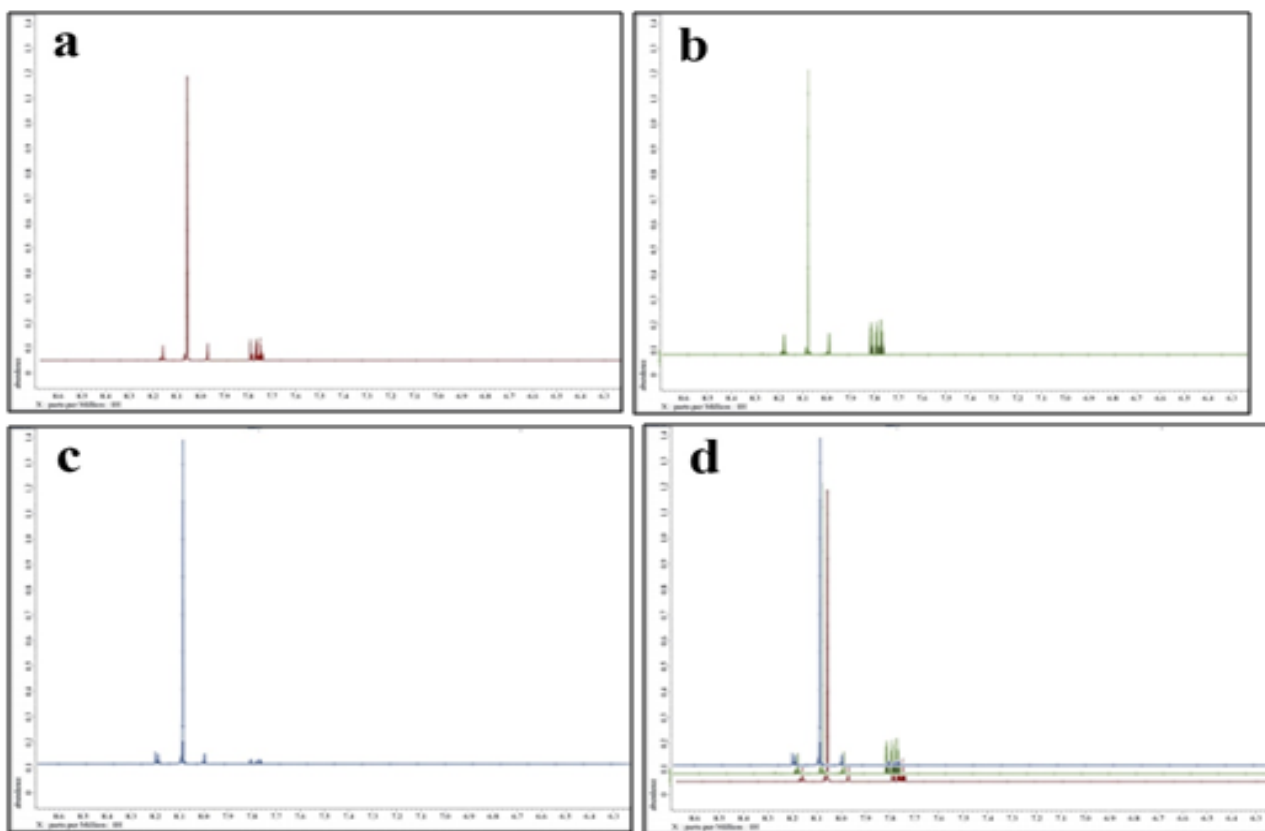


Fig 5. HNMR spectra of synthesized polycarboxylate ether, sample S31 (a), sample S32 (b), sample S33 (c), and comparison of HNMR spectra (d)

The polymers synthesized belonged to the ether group, as evidenced by the peak of C-H bond at 2800 cm^{-1} , the long peak at 1700 cm^{-1} indicating the presence of a carbonyl group, and the peak of C-O bond at 1100 cm^{-1} . Notably, no alcohol group was observed in any of the spectra. To confirm the synthesis of polycarboxylate ether, HNMR spectra were conducted, and the results are presented in Fig 5. The chemical shifts observed in the spectra included -CH₃ at 534.2 ppm, CH-CH₂CH₂ at 574.3 ppm in the side chain, and CH₂ at 352.4 ppm in the main chain. The chemical shift in the range of 5.5 ppm to 5.6 ppm was attributed to the deuterium dimethyl sulfoxide (DMSO) solution used in the analyzer. Fig 5 was presented to provide a better view of the correspondence of the diagram [29-37]. The synthesized polycarboxylate ether was subjected to the GPC analysis to determine its

characteristics. Table 4 presents the average molecular weight of the MW polymer and the molecular weight distribution of PDI. In addition, the GPC diagrams are displayed in Fig 6. The increase in MW from sample 1 to 3, ranging from 28,900 to 30,600 g/mol, can be attributed to the low reactivity of PEG at 50 °C. However, the polymerization temperature was increased to 70 °C, which provided sufficient activation energy for the reaction between AA and PEG. Finally, the slump test was conducted to verify the performance of the synthesized polycarboxylate ether. By adding 0.5% to the concrete mixture consisting of 20% Portland cement type 10, 2% water, 40% sand, and 30% sand, the obtained data in Tables 5 and 6 confirmed its performance. The confirmation of these data was made possible through the use of optical microscopy observations.

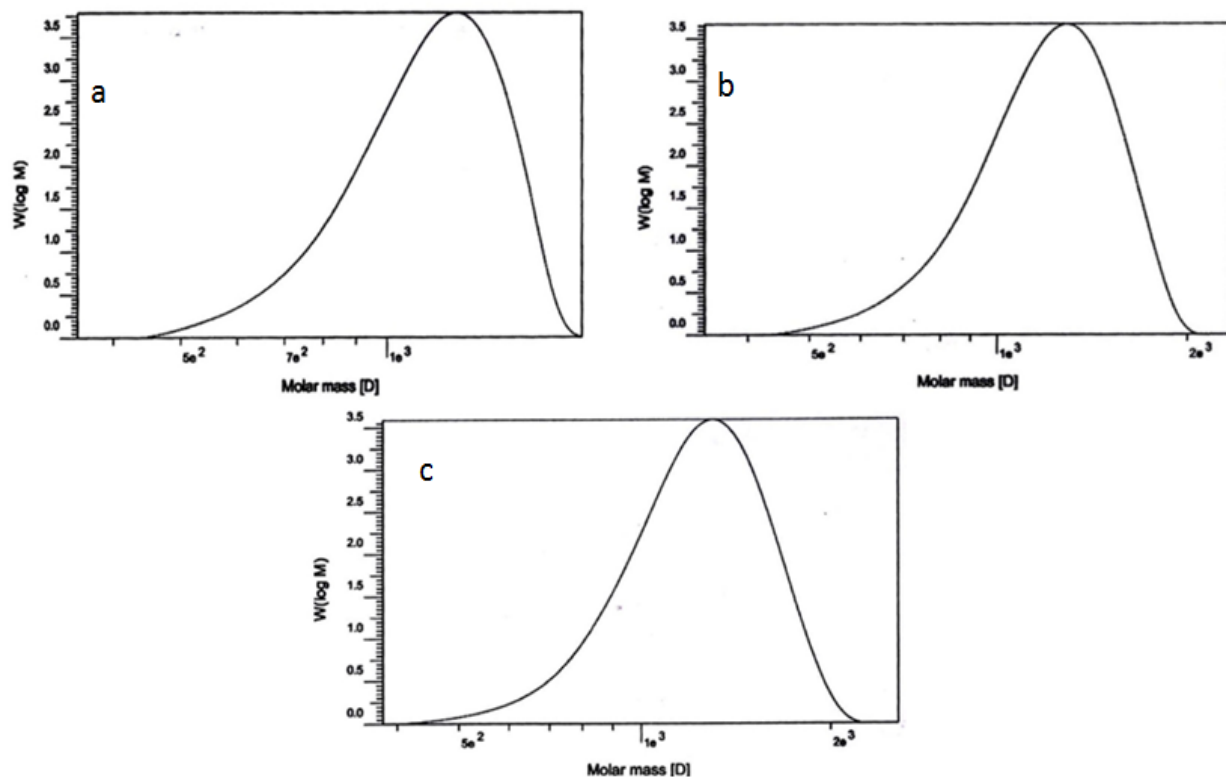


Fig 6.Gel permeation chromatogram of sample S31 (a), sample S32 (b), and sample S33 (c)

Table 4.Mix proportions of the studied samples of lime mortars

Sample	Lime:sand ratio (by volume)	Lime:sand ratio (by weight)	PCE^a (wt.%)	NS^a (wt.%)
S331	1:2	1:7.1	-	-
S332	1:2	1:7.1	0.5	-
S333	1:2	1:7.1	0.5	0.5
S334	1:2	1:7.1	0.5	1
S335	1:2	1:7.1	1	1
S336	1:2	1:7.1	2	1
S337	1:2	1:7.1	2	2

^a Values are expressed in wt.% of NS or PCE with respect to the lime weight.

^b W/B: Water/binder ratio, i.e. water/aerial lime ratio.

Table 5.Consistency, water retention, and open time of the studied mortars

Sample	Slump (mm)^a	Water retention (%)	Open time (hours)
S331	253	97.56	30.41
S332	192	95.34	32.34
S333	170	93.42	35.34
S334	167	92.42	39.42
S335	153	91.32	45.64
S336	151	91.22	47.54
S337	151	91.23	47.77

^a Consistency was assessed by means of the mini-spread flow test, which measured the slump in the flow table.

Table 6. M_w and PDI for synthesized polycarboxylate ether at different temperatures

Sample	M_w	PDI
S31	28900	2.14
S32	29100	2.14
S33	30600	1.76

In Fig 7(a), a plain lime suspension is depicted, indicating a network of portlandite particles measuring 10 μm in size, as well as agglomerates ranging from 50 to 100 μm in diameter (visible as dark spots on the micrograph). Upon closer examination in Fig 7(b), a significant population of small portlandite particles measuring 0.3 μm

can also be observed, with several areas containing multiple particles marked with white circles. These observations align with the PSD measurements. The NS introduction led to the formation of a denser and larger structure, resulting in the consumption of the smallest lime particles, as shown in Fig 7(c).

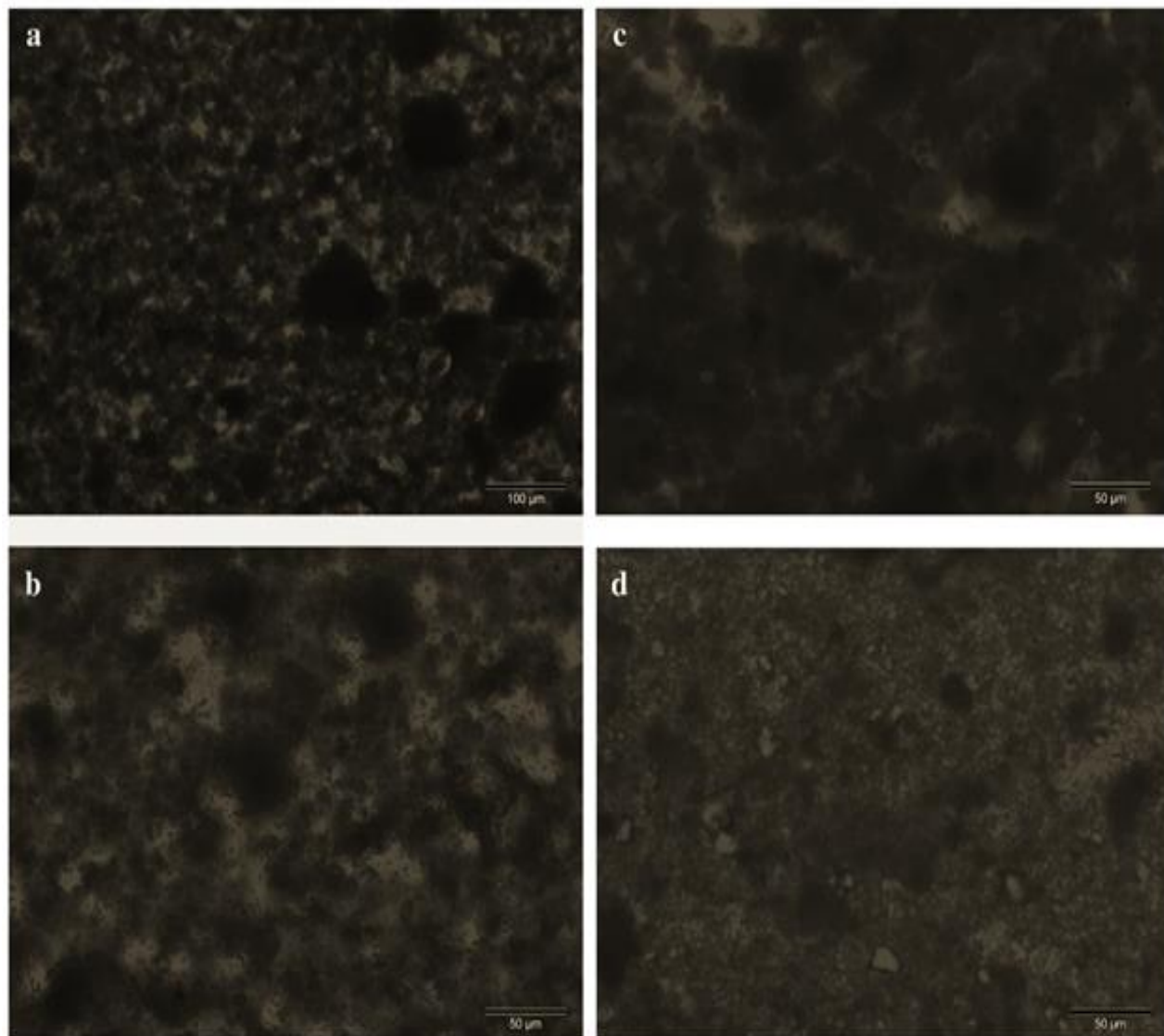


Fig 7. Optical microscopy images of lime suspensions. Large agglomerates ranging from 50 to 100 μm are indicated by white arrows (a), Image taken at a higher magnification, reveals the presence of small particles measuring 0.3 μm (b), Image shows a lime suspension mixed with NS (non-standard) material (c), and Image displays a lime-PCE (polycarboxylate ether) suspension(d)

The SEM observations enabled us to confirm a significant level of denseness in the mortar matrix in this particular case: the microstructure of the lime mortar underwent significant changes after carbonation in the presence of the PCE (Fig 8). The carbonated lime exhibited large clusters composed of tightly packed, rounded crystals of submicrometer size. The presence of PCE had a significant impact on the process of

crystal nucleation and growth, leading to the aggregation of calcite crystals. The textural properties demonstrated a decrease in porosity, while the growth of calcite crystals resulted in a more uniform and continuous matrix, facilitating the incorporation of aggregate particles. All of these alterations in the microstructure account for the enhancement in mechanical strength.

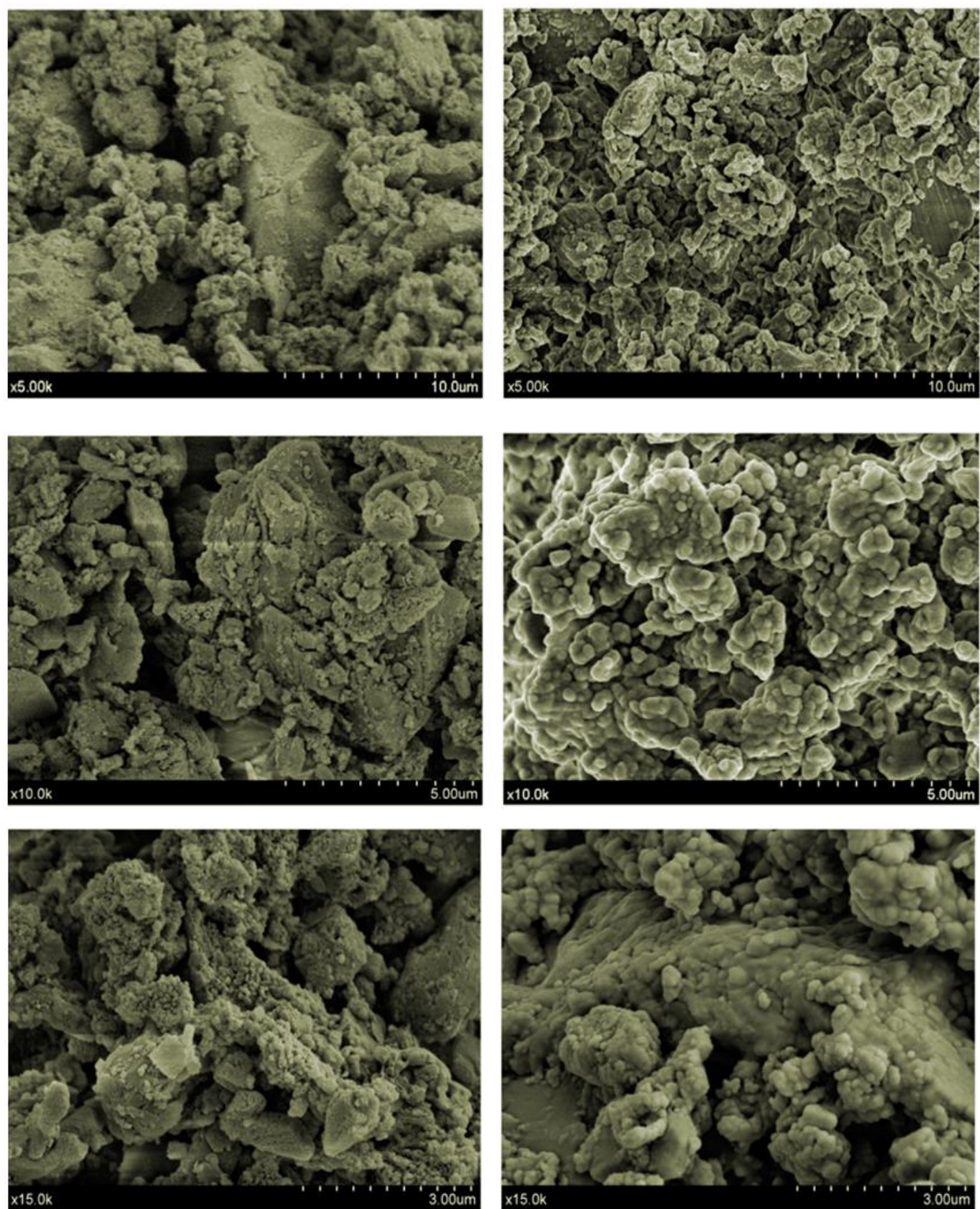


Fig 8.Comparative SEM micrographs after 7 curing days between S334 (on the left side) and S335 sample with 0.5% of plasticizer (on the right side) at different magnification. Samples with PCE showed compact and large agglomerates of rounded calcite crystals and reduced porosity

Conclusion

Based on the tests and data evaluation, the final results indicate that the length of the main chain in the copolymer increases with the rise in synthesis temperature. Moreover, this increase is more pronounced at higher temperatures. However, temperatures exceeding 70 °C lead to the degradation of the copolymer. Therefore, it is recommended to conduct the primary synthesis at a temperature of 70 °C for 8 hours. The synthesis of polycarboxylate ether with varying temperatures, while maintaining the same synthesis conditions and molar ratios of rubber, revealed that the optimal synthesis temperature is 70 °C for 6 hours. Increasing the molecular weight of polycarboxylate ether and introducing side chains result in improved slump and fluidity in concrete. One method to control the length of the main chain and side chain in polycarboxylate ether is by producing a copolymer of acrylic acid and -3-chloro-2-methyl-1-propene through the bulk method, followed by the creation of side chains using the polyethylene glycol method, which renders it soluble.

ORCID

Alireza Taheri

<https://orcid.org/0000-0003-3113-2148>

Alireza Jafari

<https://orcid.org/0000-0002-1720-7484>

Fateme Jafari

<https://orcid.org/0000-0002-3838-2193>

Funding

The authors declare that no funds, grants, or other support were received during the preparation of this manuscript.

Declarations

Conflict of interest: The authors have no relevant financial or non-financial interests to disclose.

Ethical approval: Not applicable.

Consent to participate: Not applicable.

Consent for publication: Not applicable

References

- Chuang PH, Tseng YH, Fang Y, Gui M, Ma X, Luo J. Effect of side chain length on polycarboxylate superplasticizer in aqueous solution: A computational study. *Polymers*. 2019 Feb 17;11(2):346. [Crossref], [Google Scholar], [Publisher]
- Ruijing Y, Deliang Z, Peng Z, Weide W. Research Situation on macromolecule of Polycarboxylate Superplasticizer. *J. Chem. Prod. and Tech.* 2011:32-29. [Google Scholar].
- Borget P, Galmiche L, Le Meins JF, Lafuma F. Microstructural characterisation and behaviour in different salt solutions of sodium polymethacrylate-g-PEO comb copolymers. *Colloids and Surfaces A: Physicochemical and Engineering Aspects*. 2005 Jun 15;260(1-3):173-82. [Crossref], [Google Scholar], [Publisher]
- Dongkang F, Shaozu W. He Xiaoji, Synthesis of Co-polycarboxylate Superplasticizer with Long Side Chain in Polyether and its Property, *J.* 2007;11: 42-39. [Google Scholar].
- Houst YF, Bowen P, Perche F, Kauppi A, Borget P, Galmiche L, Le Meins JF, Lafuma F, Flatt RJ, Schober I, Banfill PF. Design and function of novel superplasticizers for more durable high performance concrete (superplast project). *Cement and Concrete Research*. 2008 Oct 1;38(10):1197-209. [Crossref], [Google Scholar], [Publisher]
- Nawa T. Effect of chemical structure on steric stabilization of polycarboxylate-based superplasticizer. *Journal of Advanced Concrete Technology*. 2006;4(2):225-32. [Crossref], [Google Scholar], [Publisher]
- Winnefeld F, Becker S, Pakusch J, Götz T. Effects of the molecular architecture of

- comb-shaped superplasticizers on their performance in cementitious systems. Cement and Concrete Composites. 2007 Apr 1;29(4):251-62. [[Crossref](#)], [[Google Scholar](#)], [[Publisher](#)]
8. Ran Q, Somasundaran P, Miao C, Liu J, Wu S, Shen J. Effect of the length of the side chains of comb-like copolymer dispersants on dispersion and rheological properties of concentrated cement suspensions. Journal of colloid and interface science. 2009 Aug 15;336(2):624-33. [[Crossref](#)], [[Google Scholar](#)], [[Publisher](#)]
 9. Shentong Li, Jinzhi Liu, Yong Yang, Shuai Qi, Qianping Ran & Jiaping Liu. Synthesis, performance and working mechanism of a novel polyaryl ether superplasticizer for cement-based materials, Journal of Dispersion Science and Technology, 2020, 41:1, 1-10, [[Crossref](#)], [[Google Scholar](#)], [[Publisher](#)]
 10. LIU, Xiao, et al. Synthesis, characterization and performance of a polycarboxylate superplasticizer with amide structure. Colloids and Surfaces A: Physicochemical and Engineering Aspects, 2014, 448: 119-129. [[Crossref](#)], [[Google Scholar](#)], [[Publisher](#)]
 11. Jianhua H, Changchun W, Wuli Y. Synthesis and Mechanism of poly (carboxylate) High-range Water Reducing Agent [J]. Journal of Fudan University (Natural Science). 2000;39(4):463-6. [[Google Scholar](#)],
 12. LI S, YU Q, WEI J, JI Y. Effects of molecular mass and its distribution on adsorption behavior of polycarboxylate water reducers. Journal of the Chinese Ceramic Society. 2011 Jan 1;39(1):80-6. [[Google Scholar](#)], [[Publisher](#)]
 13. Li CZ, Feng NQ, Chen RJ. Effects of polyethylene oxide chains on the performance of polycarboxylate-type water-reducers. Cement and concrete research. 2005 May 1;35(5):867-73. [[Crossref](#)], [[Google Scholar](#)], [[Publisher](#)]
 14. Xiping L, Hui L. Influence of Side Chain Density of Polycarboxylate Superplasticizer on Hydration of Cement, J. Bulletin of the Chinese Ceramic Soc. 2009;1258-4. [[Google Scholar](#)],
 15. Baoguo M, Man Z, Hongbo T. Influence of Side Chain Density of Polycarboxylate Superplasticizer on Characteristics of Cement early Hydration, J. New Construction Materials. 2008;6:43-1. [[Google Scholar](#)],
 16. Xueqing X, Xuehong H, Yujuan H. Research of polycarboxylic copolymer side chain on the cement dispersing ability. J. Chem. Res. & Appl. 2005:828-5. [[Google Scholar](#)].
 17. SHA, Shengnan, et al. Influence of the structures of polycarboxylate superplasticizer on its performance in cement-based materials-A review. Construction and Building Materials, 2020, 233: 117257. [[Crossref](#)], [[Google Scholar](#)], [[Publisher](#)]
 18. YAMADA, Kazuo, et al. Effects of the chemical structure on the properties of polycarboxylate-type superplasticizer. Cement and concrete research, 2000, 30.2: 197-207. [[Crossref](#)], [[Google Scholar](#)], [[Publisher](#)]
 19. Xiuxing MA. Synthesis of New Polyether Polycarboxylate Superplasticizer, J. Wuhan Uni. of Tech. 2010 Oct 1:802-799. [[Crossref](#)], [[Google Scholar](#)], [[Publisher](#)]
 20. Mo XY, Yu CJ, Feng XS, Jing YJ. The Characterization and Application of Polycarboxylate as a Superplasticizer in Concrete. Advanced Materials Research. 2013 Sep 25;739:258-63. [[Crossref](#)], [[Google Scholar](#)], [[Publisher](#)]
 21. Mirzaei M. Drug discovery: a non-expiring process. Advanced Journal of Chemistry B: Natural Products and Medical Chemistry, 2020;2:46-7. [[Crossref](#)], [[Google Scholar](#)], [[Publisher](#)]
 22. Ozkendir OM. Boron activity in metal containing materials. Advanced Journal of

- Chemistry-Section B: Natural Products and Medical Chemistry, 2020;2(263):48-54. [\[Crossref\]](#), [\[Google Scholar\]](#), [\[Publisher\]](#)
23. Harismah K, Mirzaei M. Favipiravir: structural analysis and activity against COVID-19. Advanced Journal of Chemistry-Section B: Natural Products and Medical Chemistry, 2020 Jun 1;2(2):55-60. [\[Crossref\]](#), [\[Google Scholar\]](#), [\[Publisher\]](#)
24. Mirzaei, M. Lab-in-Silico Insights. Advanced Journal of Chemistry-Section B: Natural Products and Medical Chemistry, 2020; 2(1): 1-2. [\[Crossref\]](#), [\[Publisher\]](#)
25. Seyedmohammadi P, Taheri A, Rezayatizad Z. Extraction and determination of mercury from spring water, beverage and rice samples using combined microwave assisted-cloud point and dispersive-solid phase extraction in micellar media. Water and Environment Journal. [\[Crossref\]](#), [\[Google Scholar\]](#), [\[Publisher\]](#)
26. Ambarak M, Asweisi A. Determination of selenium in biological samples by flame atomic absorption spectrometry after preconcentration on modified polyurethane foam. Adv. J. Chem. Sect. B. 2020;2:10-7. [\[Crossref\]](#), [\[Google Scholar\]](#), [\[Publisher\]](#)
27. ehdi Nabati M, Pournamdari E, Dashti-Rahmatabadi Y, Sarshar S. Withaferin A (WIT) Interaction with beta-Tubulin to Promote Tubulin Degradation: In Silico Study, Advanced Journal of Chemistry-Section B: Natural Products and Medical Chemistry, 2020; 2(1): 26-32. [\[Crossref\]](#), [\[Google Scholar\]](#), [\[Publisher\]](#)
28. Kouhzadi N, Taheri A, Moafi Z. Synthesis and Characterization of Mesoporous Silica Supported Mn-Phosphomolybdate Nanocomposite for Ultra-Deep Desulfurization of Petroleum Oil Samples. Petroleum Chemistry. 2023 Jul;63(7):778-89. [\[Crossref\]](#), [\[Google Scholar\]](#), [\[Publisher\]](#)
- 29.Naghipour, B., Rahmani, V. The Combination of Remifentanil + Dexamethasone Has Favorable Effects in Management of Pain after Cesarean Section: A Systematic Review. Advanced Journal of Chemistry-Section B: Natural Products and Medical Chemistry, 2023; 5(3): 213-222. [\[Crossref\]](#), [\[Publisher\]](#)
30. Ambarak MF. Discovering of Asbestos Fibers and Corn Starch in Talc Material for Baby Powder Samples from Different Markets in Benghazi City, Advanced Journal of Chemistry-Section B: Natural Products and Medical Chemistry, 2023; 5(3): 261-270. [\[Crossref\]](#), [\[Google Scholar\]](#), [\[Publisher\]](#)
31. Branch S. A sensor for determination of tramadol in pharmaceutical preparations and biological fluids based on multi-walled carbon nanotubes-modified glassy carbon electrode. Journal of the Chemical Society of Pakistan. 2013;35:1106. [\[Google Scholar\]](#), [\[Publisher\]](#)
32. Esan, O., Bankole, O., Chrisly, O. Promethazine Hydrochloride Influence on the Micellization and the Surface Properties of Sodium Dodecyl Sulfate in Aqueous Solutions Containing Electrolytes at Various Temperatures. Advanced Journal of Chemistry-Section B: Natural Products and Medical Chemistry, 2023; 5(3): 271-288. [\[Crossref\]](#), [\[Publisher\]](#)
33. Abdollahi F, Taheri A, Shahmari M. Application of selective solid-phase extraction using a new core-shell-shell magnetic ion-imprinted polymer for the analysis of ultra-trace mercury in serum of gallstone patients. Separation Science and Technology. 2020 Oct 12;55(15):2758-71. [\[Crossref\]](#), [\[Google Scholar\]](#), [\[Publisher\]](#)
34. Mahmoodnezhad D, Taheri A. Development of a new methodology for determination of Cd, Ni, and Co at trace levels by mixed ultrasonic-assisted cloud point/solid phase extraction in micro micellar media: Optimization through response surface methodology. Journal of Food Composition

- and Analysis. 2022 Aug 1;111:104594. [Crossref], [Google Scholar], [Publisher]
35. Bozorgian, A., Ahmadpour, A. Investigating the Effect of Nanofluids in Improving the Performance of Heat Exchangers. Advanced Journal of Chemistry-Section B: Natural Products and Medical Chemistry, 2023; 5(2): 184-196. [Crossref], [Publisher]
36. Jimoh TA, Tukur A, Musa NM, Muhammad R, Obansa MI. Phytochemical and Gas Chromatography-Mass Spectrometry (GC-MS) Analysis of Ethyl Acetate Root Extract of Indigofera Diphylla, Advanced Journal of Chemistry-Section B: Natural Products and Medical Chemistry, 2023; 5(2): 173-183. [Crossref], [Google Scholar], [Publisher]
37. Nazari M, Osquee MA. Safety and Efficacy of Two Drugs, Ondansetron and Meperidine, in Preventing Shivering after Anesthesia in Orthopedic Surgery Candidates: A Systematic Review Study. Advanced Journal of Chemistry-Section B: Natural Products and Medical Chemistry, 2023; 5(2): 141-150. [Crossref],[Publisher]